Experimental study on the characteristics of the pressure drop oscillations and interaction with the short-period oscillation in a horizontal tube

Il Woong Park, Maria Fernandino, and Carlos A. Dorao*

Department of Energy and Process Engineering, Norwegian University of Science and Technology, Trondheim, Norway

Abstract

Two-phase flow instabilities have been widely studied in the literature. However, there are still open questions on the interaction between the modes of instabilities. In this work, the interaction between long-period oscillations (pressure drop oscillations) and short-period oscillations (super-imposed density wave oscillations) are studied in a horizontal heated pipe, experimentally. The different interacting modes are presented in an instability map in terms of the mass flux and the pressure drop in the heated channel. Especially, the limit cycles of the oscillations regarding on the mass flux and pressure drop obtained. The mechanism of interaction between the long-period oscillation (pressure drop oscillation) and short-period oscillation (super-imposed density wave oscillation) was identified based on obtained limit cycles in the experiments.

Research highlights

► Limit cycle for the superimposed density wave oscillation on the pressure drop oscillation is obtained from the experiment. ► The mechanism of interaction between the pressure drop oscillation and the super-imposed density wave oscillation was identified ►The boundaries between the different instability modes are identified regarding on pressure drop and subcooling.

0. Introduction

A considerable amount of studies on two-phase flow instabilities has been conducted during the past decades (Boure et al., 1973; Durga Prasad et al., 2007; Kakac and Bon, 2008; Liang et al., 2010; Tadrist, 2007) due to its relevance to refrigeration, steam generator, boiling water reactor, and etc. The main issue of the instabilities are the oscillations in temperature, flow, and pressure which can cause thermal fatigue, mechanical vibration, deterioration of heat transfer, and difficulty of control of the system.

Among the type of the two-phase flow instabilities, a pressure drop oscillation (PDO) is characterized by a long period of oscillation. This is important phenomenon since it could trigger dry out in the multi-channel configuration (Kandlikar, 2002). The essential conditions for the occurrence of the PDOs were discussed in (Boure et al., 1973; Padki et al., 1992) which can be summarized like: the system has a compressible volume, the internal system characteristic curve presents a negative slope of the N-shape curve in terms of pressure drop versus flow rate curve, and the external characteristic curve steeper than an internal characteristic curve. PDOs have been studied theoretically (Doğan et al., 1983; Mawasha et al., 2001; Padki et al., 1992, 1991; Stenning and Veziroglu, 1965) and experimentally (Çomaklı et al., 2002; Ding et al., 1995; Guo et al., 1996; Ozawa et al., 1979; Yüncü et al., 1991) in the past decades. Recent studies on PDO have been reported in the condition of the mini channel (Yu et al., 2016) and microchannel system (Zhang et al., 2010). However, due to the complexity of the process, the mechanisms controlling the characteristics of the PDO and the impact of the oscillations in the heat transfer and pressure drop remain major research challenges. Manavela et al. (Manavela Chiapero et al., 2012) have summarized previous studies and the remaining challenges on PDOs. Moreover, it has been discussed that the effect of different parameters on the N-shape curve which are critical to pressure drop oscillation by Manavela Chiapero et al., (2013).

In the case of horizontal pipes, parametric studies have been done to determine the effect of various parameters on the period and amplitude (Çomaklı et al., 2002; Ding et al., 1995; Yüncü et al., 1991). However, there are discrepancies between the previous studies regarding the effect of experimental conditions on the period and the amplitudes of PDO. Çomaklı et al., (2002) and Ding et al., (1995) have observed that the amplitude and period increases with increasing mass flux, while Yüncü et al., (1991) has reported that the mass flux has no effect on amplitude and the period decreases at lower mass fluxes and increases with increasing mass flux. They also reported a stability maps which show the condition for the instabilities. PDO was mostly observed in negative slope regions of the N-shape curve in previous studies but PDO in the positive slope region was reported by Çomaklı et al., (2002). Furthermore, the boundaries for the PDO were given in terms of inlet temperature and mass flux where both left and right boundaries of mass flow rate shift to higher mass flow rate with increasing inlet temperature.

Under given conditions, the PDOs can show a superimposed high-frequency oscillation (Çomaklı et al., 2002; Ding et al., 1995; Yüncü et al., 1991). This high-frequency oscillation has been attributed to be density wave oscillations (DWO) triggered at the lowest region of the flow rate oscillation. Studies on the interaction between the PDO and DWO have been performed both experimentally (Liu and Kakac, 1991) and numerically (Schlichting et al., 2010; Yin et al., 2006). It has been observed that the DWO can be superimposed in the PDO when the slope of the internal characteristic curve is negative (Liu and Kakac, 1991). It has been assumed that the DWO occurs during the passing through the left positive slope in the limit cycle causing a violent oscillation of the mass flux. Numerical studies have shown that the oscillations mode changes in the sequence of pure DWO, transition, PDO with DWO, and pure PDO by increasing mass flux with constant inlet temperature condition (Yin et al., 2006). Remarkably, it has been reported that after the PDO with DWO region, there is the pure PDO region which was not observed in previous experimental studies.

The mechanism for the PDO and the superimposed DWO were explained with a limit cycle in previous studies as shown in Figure 1 (Liu and Kakac, 1991; Manavela Chiapero et al., 2012; Schlichting et al., 2010). The process for a PDO can be summarized as a compression in the surge tank (A1-B), a flow excursion to liquid phase (B-C1), a decompression in the surge tank (C1-D), and a flow excursion to gas phase (D-A1). The mechanism of the super-imposed density wave oscillation was explained that the superimposed DWO occurs in rising part of the pressure drop (A-B) due to the boiling which makes the oscillation violent by Liu and Kakaç (1991) as shown in Figure 1a. Schlichting et al. (2010) presented an analysis of the interaction between the PDO and DWO by using a transient lumped parameter model. As shown in figure 1b, it has been observed that the interactions between super-imposed oscillation and pressure drop oscillation could be richer than previous studies. However, it was observed that the limit cycle was not developed along the internal system characteristic curve in the given condition for the analysis. The shape of the limit cycle can be important to understand the underlying the mechanism of the interaction between the pressure drop oscillations and short-period oscillations. It could be expected that the limit cycle has characteristics of the hypothetical explanation by Liu and Kakaç (1991) and the analysis by Schlichting et al. (2010). The limit cycle would follow the internal characteristic curve during the phase of a flow excursion to liquid phase, a decompression in the surge tank, and a flow excursion to the gas phase. After the flow excursion to the gas phase, it would have large fluctuations of mass flux as observed by Schlichting et al. (2010) during the phase of the compression in the surge tank.

In summary, different types of the two-phase instabilities and the interaction between them in conditions with different channel configurations have been observed during the past decades. However, there are still many open questions on two-phase instabilities and also the interaction between the two-phase flow instabilities.

In this study, the effect on the period and amplitude with different mass flux and subcooling are experimentally studied with the goal of the study for the mechanisms controlling the interaction between long-period oscillations (pressure drop oscillations) and short-period oscillations (super-imposed density wave oscillations). Limit cycles for the pressure drop oscillation are obtained in order to improve understanding of the mechanism of superimposed high order oscillation and the interaction between different modes of instabilities.

2. Material and Method

2.1 Experimental facilities

The experimental facility for two-phase flow instability test consists of a closed main loop, a tank, a pump, a conditioner, a condenser, a test section, two flow meters, two chillers, and a visualization glass as shown in Figure 2. R134a is used as a working fluid and a magnetically coupled gear pump is located between the main tank and the conditioner. The pressure and the temperature of the main loop are mainly controlled by the saturated conditions in the main tank. The conditions of working fluid in the main tank are controlled by chillers connect to the condenser and conditioner in order to reach stable the experimental conditions. The inlet fluid temperature and outlet fluid pressure are adjusted by two chillers connected to the conditioner and the condenser. Two Coriolis flow meters are located before the surge tank (G_1) and after the surge tank (G_2) for measuring the flow. The surge tank is located above the closed main loop and it is connected to before the test section. It has a 219 mm of diameter and 9.5 × 10-3m^3 of volume. It is filled with R134a and nitrogen gas. The pressure and level of the surge tank are controlled by a nitrogen tank which is connected to the top of the surge tank. There is a manually operated valve between the surge tank and main loop in order to trigger the pressure drop oscillations.

The test section which is a stainless steel tube has 5mm of the inner diameter and 8mm of the outer diameter and 2035mm of the length. The schematic diagram of the heated channel is

described in Figure 3. The test section is heated electrically by electrodes in five independent sections and power input of the each section are controllable. There are 7 pressure taps inside the test section in order to measure pressure drop inside the channel. 9 and 11 of thermocouples are installed on top and bottom of the test section. In each position 6 and 10, there are two more thermocouples in both sides of the wall between thermocouples on top and bottom. The temperatures of the fluid are obtained in position 6 and 10. The variables of temperature and pressure are logged with a National Instruments (NI) data acquisition system.

2.2 Measurements and accuracy

For the temperature measurements, 0.5 mm diameter of T-type thermocouples have been used and it has 0.1K of accuracy (in-house calibration). A saturation temperature of the working fluid is determined by the absolute pressures. Pressures at the inlet and the outlet of the test section are measured by absolute pressure transducers. They have a 0.04% of accuracy at 2.5 MPa of full-scale. A pressure drop between inlet and outlet of the test section is measured by differential pressure transducers. It has a 0.075% of accuracy at 0.05 MPa of full-scale. A mass flow rate has a 0.2% of accuracy. The accuracies of absolute pressure, pressure drop, and mass flow rate are given by the supplier. Heat flux is calibrated by means of heat transfer to the fluid in a stationary condition. It was compared the electrical power and a heat transfer between single-phase liquid and surrounding. The accuracy of 3% is derived for the heat flux. The vapour quality along the test section is calculated based on a heat balance.

2.3 Experimental procedure and conditions

As a first step of the experimental procedure, the pump was started. In this step, sufficient flows were supplied for avoiding dry out in the test section. After obtaining a stable flow condition, a 35kW/m^2 of a heat flux was gradually applied to the test section. By controlling the temperatures

of the liquid in chillers which are connected to the conditioner and the condenser, the inlet pressure (700 kPa) and subcooling temperature (35.0, 37.5, and 40.0 K) were adjusted. And also the inlet mass flux (400–2000 kg/m^{2}s) was adjusted by controlling the pump speed. Regarding on the experimental condition, it was not possible to reach the experimental condition for the low mass flux (<500 kg/m^{2}s) with high subcooling temperature (40 K). That was because the minimum temperature (253.15 K) of the chiller connected to conditioner was not low enough in order to maintain high subcooling temperature in a given condition. By adjusting temperatures of the chillers and the pump speed, desired conditions were obtained for each test cases. After this, the pressure drop oscillation was introduced by opening the valve between the surge tank and the test section. Table 1 shows a comparison of experimental condition between the previous experimental studies on pressure drop oscillation in a horizontal channel.

For triggering the pressure drop oscillation, it was essential to obtain a negative slope in the internal system characteristic curve. Figure 4a and 4b show the internal system characteristic curves for the test section and the main flow loop for three different subcooling temperature. Negative slopes were observed in each subcooling temperature. For obtaining the internal system characteristic curve, the flow rate was decreased in stepwise while the inlet pressure and subcooling temperature were maintained as constant by controlling the temperature of two chillers. The pressure drop in the main loop (ΔP_{system}) is obtained from the difference between the pressure after the pump (P_P) and the before the main tank (P_B). The pressure drop in the test section (ΔP_{TS}) is measured by the difference between the pressure before the test section (P_{in}) and after the test section (P_{out}).

3. Results and discussion

3.1 different modes of instabilities

Figure 5 shows the test conditions of inlet mass flux on the x-axis and subcooling temperatures on the y-axis. Different oscillation modes namely: no oscillation, decreasing long-period oscillation, long-period oscillation, and long-period oscillation followed by short-period oscillation, were observed and they are depicted with different symbols and the hypothetical boundaries are sketched. It was observed that long-period oscillation followed by short-period oscillation is taken place with high subcooling temperature in the case of 37.5 K and 40.0 K of subcooling temperature. The decreasing long-period oscillation mode was located in the high mass flux region between long-period oscillation and no oscillation regions. No oscillation was observed in both low mass flux and high mass flux region.

In terms of inlet temperature and mass flow rate, the trend of boundaries for the long-period oscillation shows a similar result compared to the ones from the previous study by Çomaklı et al. (2002). It was reported that both left and right boundaries in mass flow rate shifted to higher mass flow rate with increasing inlet temperature. In this study, it was shown that both sides of boundaries in inlet mass flux shifted to higher mass flow rate when the inlet subcooling temperature decreases.

It has been observed that the density wave oscillation was super-imposed on the pressure drop oscillations in previous studies (Çomaklı et al., 2002; Ding et al., 1995; Yüncü et al., 1991). An existence of long-period oscillation without short-period oscillation or a distinctive classification of the long-period oscillation and long-period oscillation with short-period oscillation were not reported in the previous experimental studies. However, not only an existence of the long-period oscillation but also a mode change between the long-period oscillations to long-period oscillation followed by short-period oscillation were observed in this study. This mode change was reported in the previous study analytically by Yin et al. (2006) that the instabilities mode changes as the following sequence that DWO, transition, PDO with DWO, and PDO with increasing mass flux and

constant subcooling analytically. It could be concluded that PDO with DWO to PDO among those mode changes was demonstrated experimentally in this study.

Figure 6 shows that the boundaries for the different oscillation mode on the characteristic curves where the total pressure drop is the sum of the pressure drop in test section and the pressure drop in the system. No oscillation was observed when the slope of the N-shape curve becomes positive after the negative slope region. Yin et al. (2006) reported that the region for the superimposed DWO with PDO instability occurs when the system has a higher pressure drop and a steeper negative slope of the internal characteristic curve. However, it was observed that the long-period oscillation followed by short-period oscillation occurs with steeper negative slope and low-pressure drop condition in this study. Based on observation from both analytical and experimental studies, it could be concluded that the steepness of the negative slope of the internal characteristic curve is more critical than the pressure drop.

Figure 7 and 8 show the trend of the pressure and the mass flux for each oscillation mode in the condition of 40.0 K of subcooling. Initial mass fluxes (G_i) for each case are described in each graph. In figure 7, the pressure at the inlet (Pin, blue solid line) and outlet (Pout, red dash line) of the test section are depicted. In figure 8, the mass flux before the surge tank (G_1, red dash line) and between the surge tank and test section (G_2, blue solid line) are described. Figure 7a and 8a represent the stable mode. In this case, there was no specific reaction after opening the valve for triggering the instability. Figure 7b and 8b represent decreasing long-period oscillation mode. It was characterized with decreasing amplitude of oscillations as time goes by. Figure 7c and 8c show the long-period oscillation. In this mode, the pressure and mass flux oscillated continuously. Figure 7d and 8d show the long-period oscillation followed by short-period oscillation mode. The short-period oscillation between the long-period oscillations was observed in both pressure and mass flux.

3.2 Limit cycles for the different oscillation modes

Limit cycles for the different oscillation modes are depicted in Figure 9. Initial mass flux (G_i) and subcooling temperature are described in each graph. It was possible to observe the behavior of short-period oscillation followed by long-period oscillation. There were two types of short-period oscillations which occurred in the middle of negative slope and top of the negative slope. It was observed that the pressure drop passed over the first point of inflection in the internal characteristic curve in case of long-period oscillation with short-period oscillation. On the contrary, the pressure drop wasn't overshot over the first point of inflection in the internal characteristic curve when there is no superimposed short-period oscillation. For the case of 35.0 K of inlet subcooling, both mass flux before the surge tank (G_1) and mass flux after the surge tank (G_2) are depicted. It was observed that the limit cycle of the G_1 represents the external characteristic curve. It was shown that the long-period oscillation was not maintained when the external characteristic curve crossed the second point of inflection in the internal characteristic curve. It shows that the negative slope of the internal characteristic curve is essential for maintaining pressure drop oscillation, even though the slope of the external characteristic curve was steeper than that of the internal characteristic curve.

A synchronized data of pressure drop and mass flux for the limit cycle in the case of superimposed short-period oscillation was obtained in this study. It can be depicted in schematic diagram as described in Figure 10. It was observed that the short-period oscillation occurred before the end of the flow excursion to the gas phase. And there were two types of short-period oscillation which are first short-period oscillation (A*-B*) and second short-period oscillation (B*-C*). It can be classified by the criteria which are the point of the inflection in the internal characteristic curve. In the case of second oscillation, it occurred at the inflection point and the fluctuation reached to negative mass flux and out of the internal characteristic curve. During this second oscillation, there was an overshoot of pressure drop (B*-C*) compared with a previous explanation for the

mechanism of PDO. It could be explained that when the flow reaches the inflection point (B*) the sudden flow excursion compared to typical PDO occurred and it caused the overshoot of the mass flux. After this, it continued because of the inertia force which makes fluctuations until the start of the depression of the surge tank process. However, it is not well-known when the superimposed short-period oscillation triggered. They could be yield because of the low mass flux or the fast flow excursion from low quality to high quality. It was shown that the flow excursion to the liquid phase was not fully relaxed (C*-D*), it could be explained that it was because a compressible volume was not large enough and the thermal capacity was not small enough. And it was observed that after the flow excursion from the two-phase to a liquid phase, the flow didn't reach to complete liquid phase due to the high heat flux condition. In summary, the limit cycle following the internal characteristic curve was observed in the phase of C*-D*- A*, the high fluctuation of mass flux was observed in the phase of A*-B*, and an overshoot of the pressure drop was newly observed in the phase of B*-C*.

3.3 Effect of subcooling temperature and mass flux

In order to clarify the discrepancies on the effect on amplitude and period between the previous studies, both amplitude and period are measured for the test cases. The average of peak to peak amplitude per mean value of the mass flux are derived as amplitude. Only long period oscillations are considered and short period oscillations are not considered for calculating the amplitude of the oscillations. Decreasing long-period oscillation is considered as a zero amplitude of oscillation in order to clarify the effect on amplitude. An inlet pressure, a heat flux, volume of liquid in the surge tank, and pressure in surge tank are controlled as constant in every case.

The effect of subcooling temperature and mass flux on amplitude and period are depicted in Figure 11. In figure 11a, the x-axis which is a normalized amplitude represents the peak-to-peak

amplitude per mean of the flow. The amplitude of the oscillation increases with increasing mass flux until certain mass flux. After that, the amplitude of the oscillation decreases. The period of oscillation increases with increasing mass flux. In the case of subcooling temperature, as subcooling temperature increases the amplitude of oscillation is increased in the low mass flux region. However, the amplitude of oscillation decreases with increasing subcooling temperature in the high mass flux region. As subcooling temperature increasing, the mass flux which has a maximum amplitude of PDO is decreasing. As depicted in figure 11b, the period of PDO increases with increasing mass flux and also subcooling temperature. The effect on the amplitude and period of the oscillation is summarized, including previous studies (Çomaklı et al., 2002; Ding et al., 1995; Yüncü et al., 1991) as described in Table 2. Regarding amplitude of oscillation, it is newly observed in the experiment that the increment of amplitude and decrement of amplitude following increment of amplitude as an increasing mass flux. After the peak of the amplitude of oscillation, the limited cycle of oscillation becomes smaller and it shows the decrease in the amplitude. Those discrepancies could come from the different method for triggering oscillation and the configuration of the flow loop.

4. Conclusion

In the present study, the experiment was conducted for clarifying the mechanism for the oscillation mode changes. The region of decreasing amplitude of oscillation with increasing mass flux in high mass flux condition was newly observed. The boundaries for the four type of instability modes were derived in terms of pressure drop and subcooling temperature. It was concluded that the critical variable for the existence of the superimposed short-period oscillation is the steepness of the negative slope of the internal characteristic curve. The limit cycle was obtained for explaining the superimposed short-period oscillations. A schematic diagram was presented based on the experimental data for explaining pressure drop oscillation with super-imposed short-period

oscillations. A remarkable point is that the overshoot of the pressure drop over the internal characteristic curve was newly observed in the case of the long-period oscillation with short-period oscillation.

Corresponding Author

* E-mail: carlos.dorao@ntnu.no

Acknowledgments

The Ph.D. fellowship (Il-Woong Park) financed by the NTNU-SINTEF Gas Technology Centre is gratefully acknowledged.

References

Boure, J.A., Bergles, A.E., Tong, L.S., 1973. Review of Two-Phase Flow Instability. Nucl. Eng. Des. 25, 165–192.

Çomaklı, Ö., Karslı, S., Yılmaz, M., 2002. Experimental investigation of two phase flow instabilities in a horizontal in-tube boiling systems. Energy Convers. Manag. 249–268.

Ding, Y., Kakac, S., Chen, X.J., 1995. Dynamic Instabilities of Boiling Two-Phase Flow in a Single Horizontal Channel 1777, 327–342.

Doğan, T., Kakaç, S., Veziroğlu, T.N., 1983. Analysis of forced-convection boiling flow instabilities in a single-channel upflow system. Int. J. Heat Fluid Flow 4, 145–156. doi:10.1016/0142-727X(83)90060-7

Durga Prasad, G. V., Pandey, M., Kalra, M.S., 2007. Review of research on flow instabilities in natural circulation boiling systems. Prog. Nucl. Energy 49, 429–451. doi:10.1016/j.pnucene.2007.06.002

Guo, L.J., Feng, Z.P., Chen, X.J., Thomas, N.H., 1996. Experimental Investigation of Forced Convective Boiling Flow Instabilities in Horizontal Helically Coiled Tubes. J. Therm. Sci. 5, 210–216.

Kakac, S., Bon, B., 2008. A Review of two-phase flow dynamic instabilities in tube boiling systems. Int. J. Heat Mass Transf. 51, 399–433. doi:10.1016/j.ijheatmasstransfer.2007.09.026

Kandlikar, S.G., 2002. Two-Phase Flow Patterns , Pressure Drop , and Heat Transfer during Boiling in Minichannel Flow Passages of Compact Evaporators. Heat Transf. Eng. 23.1, 5–23.

Liang, N., Shao, S., Xu, H., Tian, C., 2010. Instability of refrigeration system – A review. Energy Convers. Manag. 51, 2169–2178. doi:10.1016/j.enconman.2010.03.010

Liu, H.T., Kakac, S., 1991. An experimental investigation of thermally induced flow instabilities in a convective boiling upflow system. Heat Mass Transf. 26, 365–376. doi:10.1007/bf01591669

Manavela Chiapero, E., Fernandino, M., Dorao, C. a., 2013. On the influence of heat flux updating during pressure drop oscillations - A numerical analysis. Int. J. Heat Mass Transf. 63, 31–40. doi:10.1016/j.ijheatmasstransfer.2013.03.047

Manavela Chiapero, E., Fernandino, M., Dorao, C. a., 2012. Review on pressure drop oscillations in boiling systems. Nucl. Eng. Des. 250, 436–447. doi:10.1016/j.nucengdes.2012.04.012

Mawasha, P.R., Gross, R.J., Quinn, D.D., 2001. Pressure-Drop Oscillations in a Horizontal Single Boiling Channel. Heat Transf. Eng. 22, 26–33. doi:10.1080/01457630152496296

Ozawa, M., Nakanishi, S., Ishigai, S., Mizuta, Y., Tarui, H., 1979. Flow Instabilities in Boiling Channels: Part 1 Pressure Drop Oscillations. Bull. JSME Vol. 22, 1113–1118.

Padki, M.M., Liu, H.T., Kakac, S., 1991. Two-phase flow pressure-drop type and thermal oscillations. Int. J. Heat Fluid Flow 12, 240–248. doi:10.1016/0142-727X(91)90058-4

Padki, M.M., Palmer, K., Kakaç, S., Veziroğlu, T.N., 1992. Bifurcation analysis of pressure-drop oscillations and the Ledinegg instability. Int. J. Heat Mass Transf. 35, 525–532. doi:10.1016/0017-9310(92)90287-3

Schlichting, W.R., Lahey, R.T., Podowski, M.Z., 2010. An analysis of interacting instability modes, in a phase change system. Nucl. Eng. Des. 240, 3178–3201. doi:10.1016/j.nucengdes.2010.05.057

Stenning, A.H. (University of M., Veziroglu, T.N., 1965. Flow oscillation modes in forced-convection boiling, in: Heat Transfer and Fluid Mechanincs Institute. NASA Grant NsG-424. pp. 301–316.

Tadrist, L., 2007. Review on two-phase flow instabilities in narrow spaces. Int. J. Heat Fluid Flow 28, 54–62. doi:10.1016/j.ijheatfluidflow.2006.06.004

Yin, J., Lahey Jr., R.T., Podowski, M.Z., Jensen, M.K., 2006. An analysis of interacting instability. Multiph. Sci. Technol. 18, 359–385.

Yu, Z., Yuan, H., Chen, C., Yang, Z., Tan, S., 2016. Two-phase flow instabilities of forced circulation at low pressure in a rectangular mini-channel. Int. J. Heat Mass Transf. 98, 438–447. doi:10.1016/j.ijheatmasstransfer.2016.03.047

Yüncü, H., Yildirim, O.T., Kakac, S., 1991. Two-phase flow instabilities in a horizontal single boiling channel. Appl. Sci. Res. 48, 83–104.

Zhang, T., Peles, Y., Wen, J.T., Tong, T., Chang, J.-Y., Prasher, R., Jensen, M.K., 2010. Analysis and active control of pressure-drop flow instabilities in boiling microchannel systems. Int. J. Heat Mass Transf. 53, 2347–2360. doi:10.1016/j.ijheatmasstransfer.2010.02.005

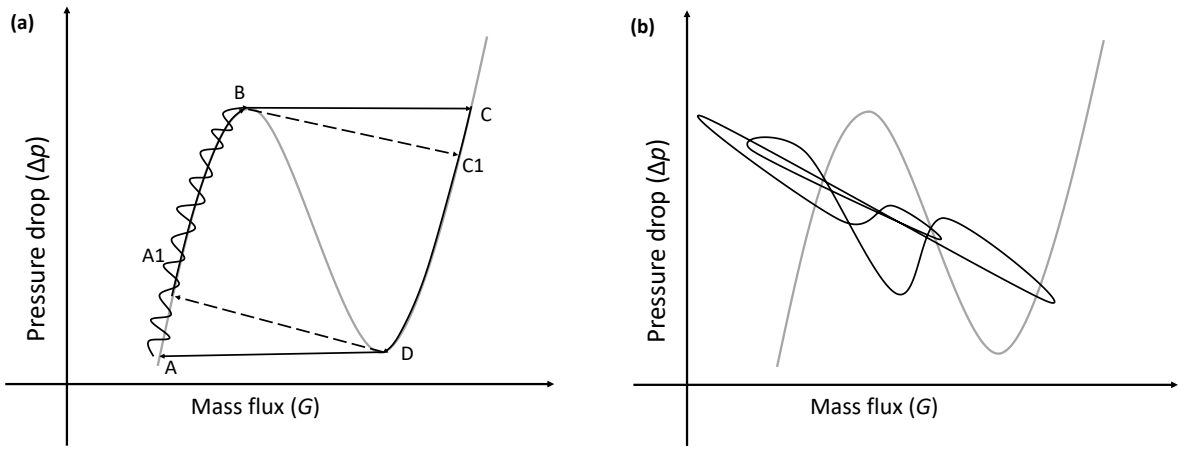

Figure 1. Schematic diagram of limit cycle for the PDO (Manavela Chiapero et al., 2012) and the interaction between long-period oscillations and short-period oscillations in previous study (a) (Liu and Kakac, 1991), (b) (Schlichting et al., 2010)

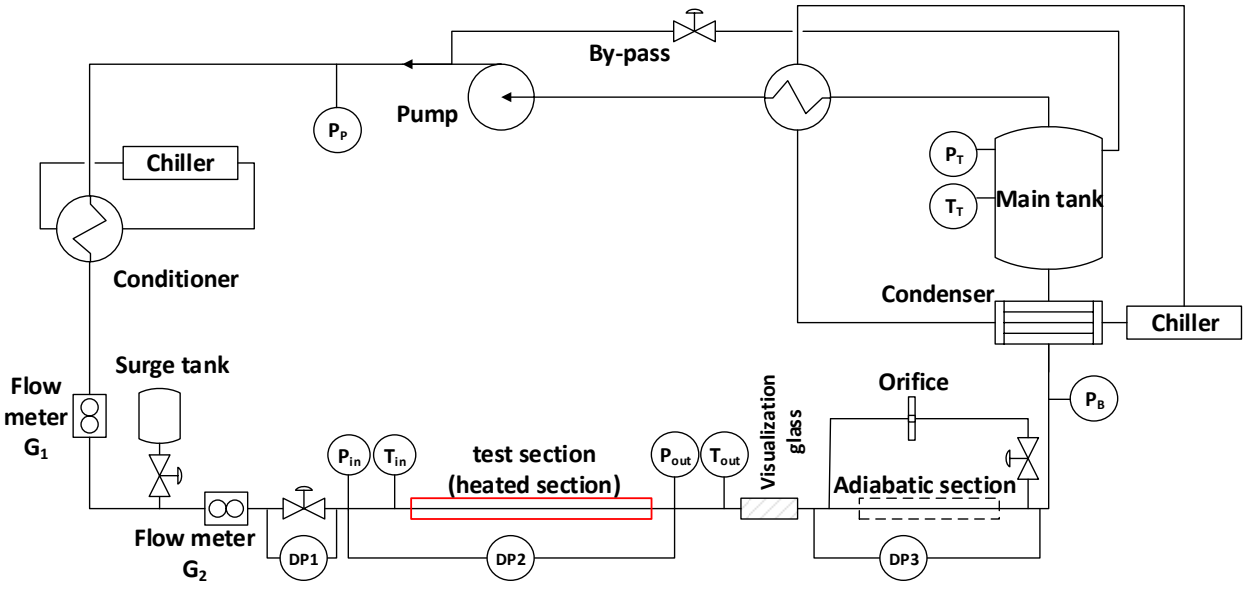

Figure 2. Schematic diagram of the test facility.

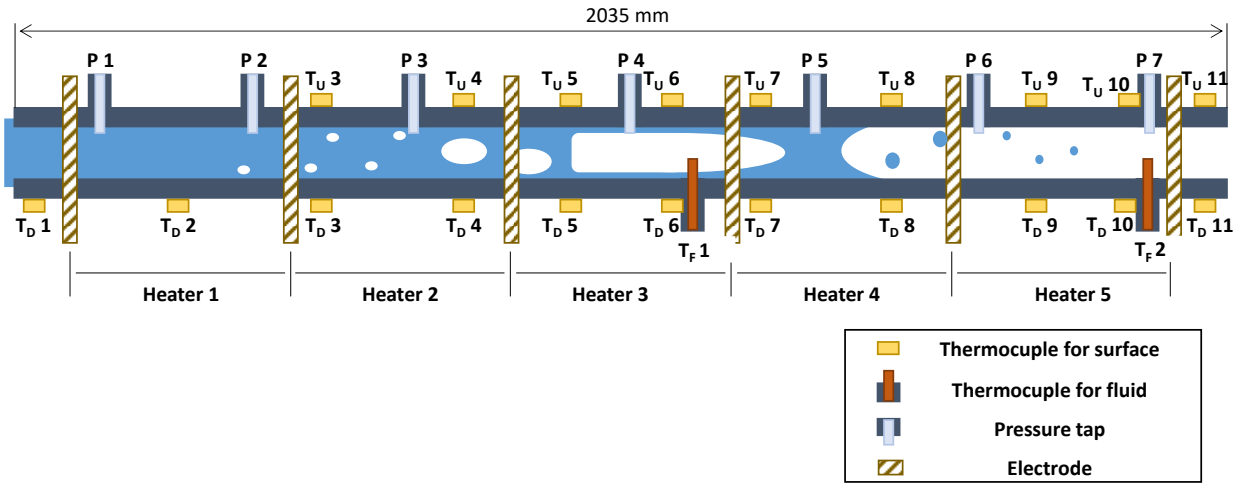

Figure 3. Schematic diagram of the test section.

Table 1. A comparison of experimental conditions

Parameter	Yüncü et al., 1991	Çomaklı et al., 2002	Ding et al., 1995	Park et al.
Fluid	R-11	R-11	R-11	R-134a
Inner diameter of test section	5 mm	11.2 mm	10.9 mm	5 mm
Length of test section	800 mm	3500 mm	1060 mm	2035 mm
System pressure	686000 Pa	750000 Pa	760000 Pa	700000 Pa
Mass flux (where PDO obtained)	200 – 560 kg/m^{2}s	365 – 731 kg/m^{2}s	240 – 900 kg/m^{2}s	400 – 1000 kg/m^{2}s
Heat flux	23 – 40 kW/m^2	121 kW/m^2	55 – 76 kW/m^2	35 kW/m^2
Inlet temperature	20 °C	16 – 28 °C	2 – 24 °C	-12 – -8 °C
Compressible volume	0.0084 m^2	0.05 m^3	0.0021 m^3	0.00471 m^3

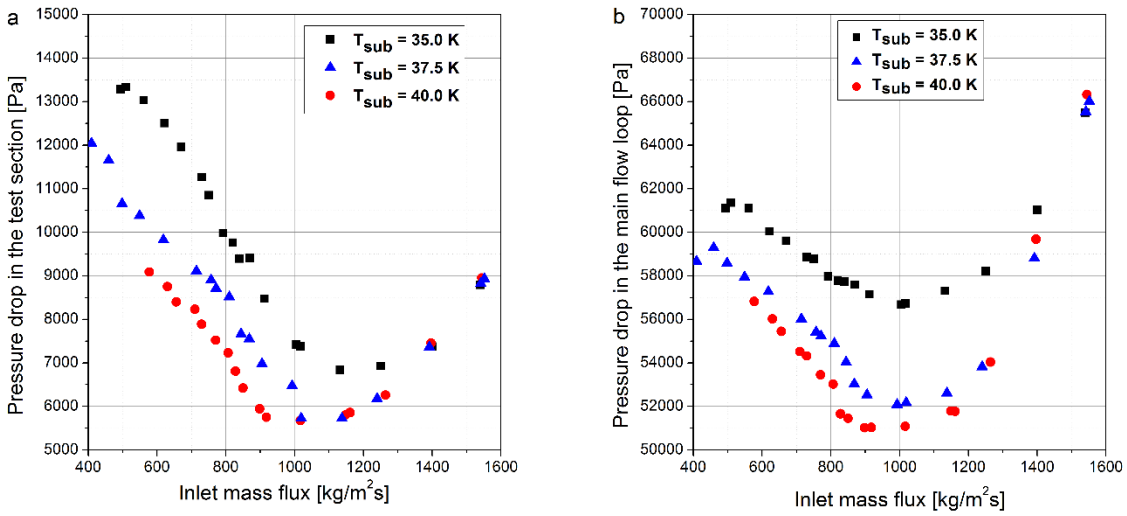

Figure 4. N-shape curve of the test section (a) and main flow loop (b)

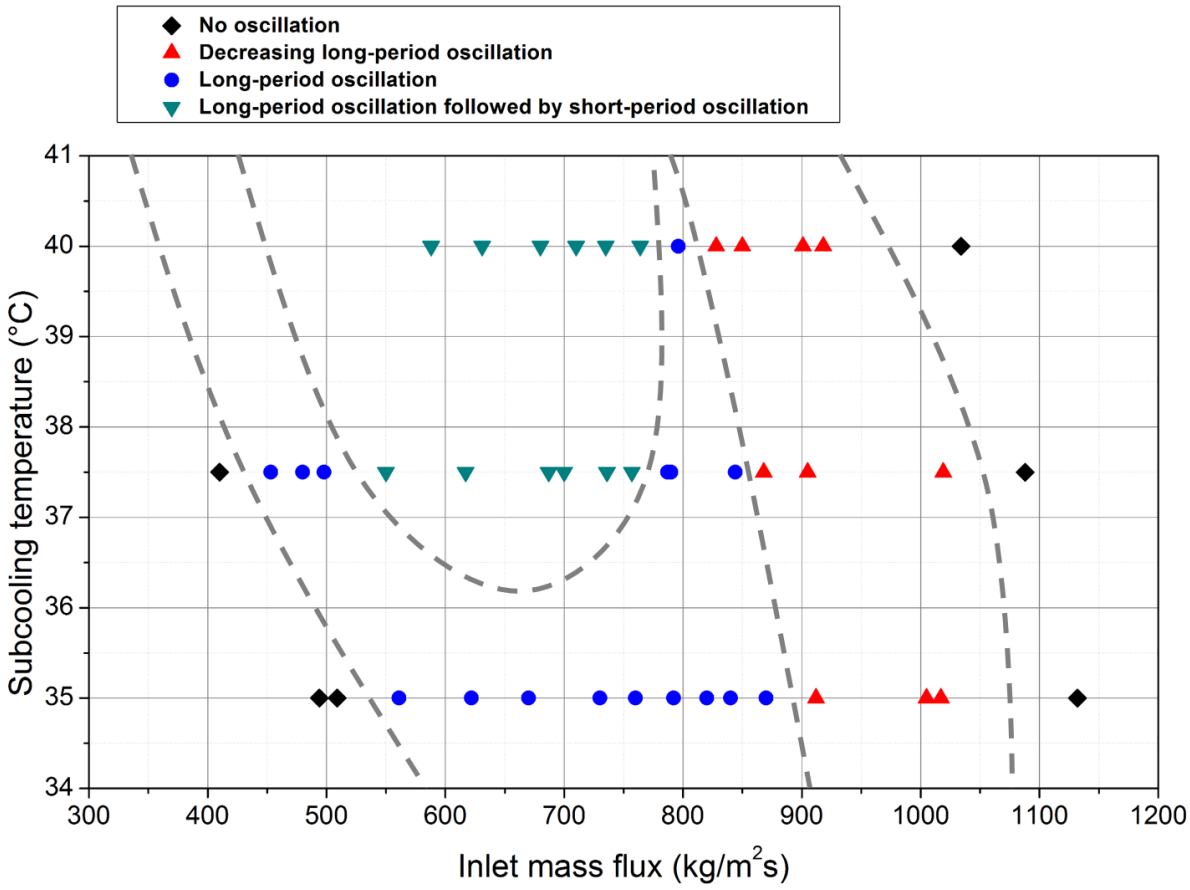

Figure 5. Boundaries for the different instabilities modes (Subcooling)

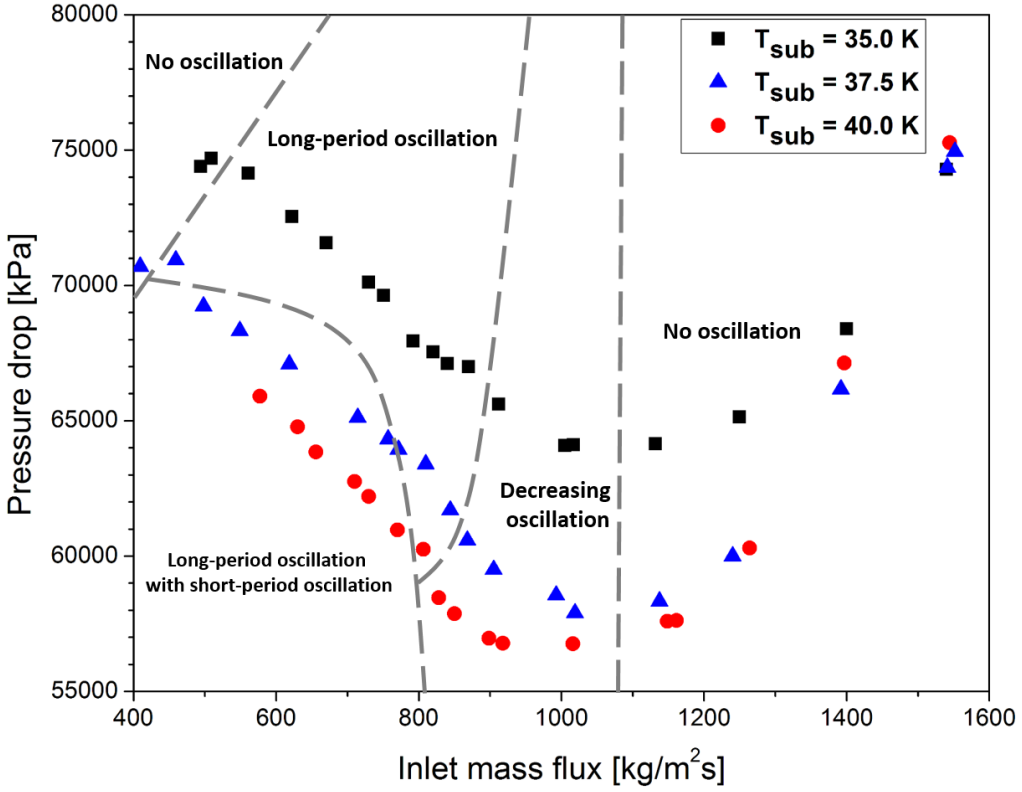

Figure 6. Boundaries for the different instabilities modes (characteristic curves)

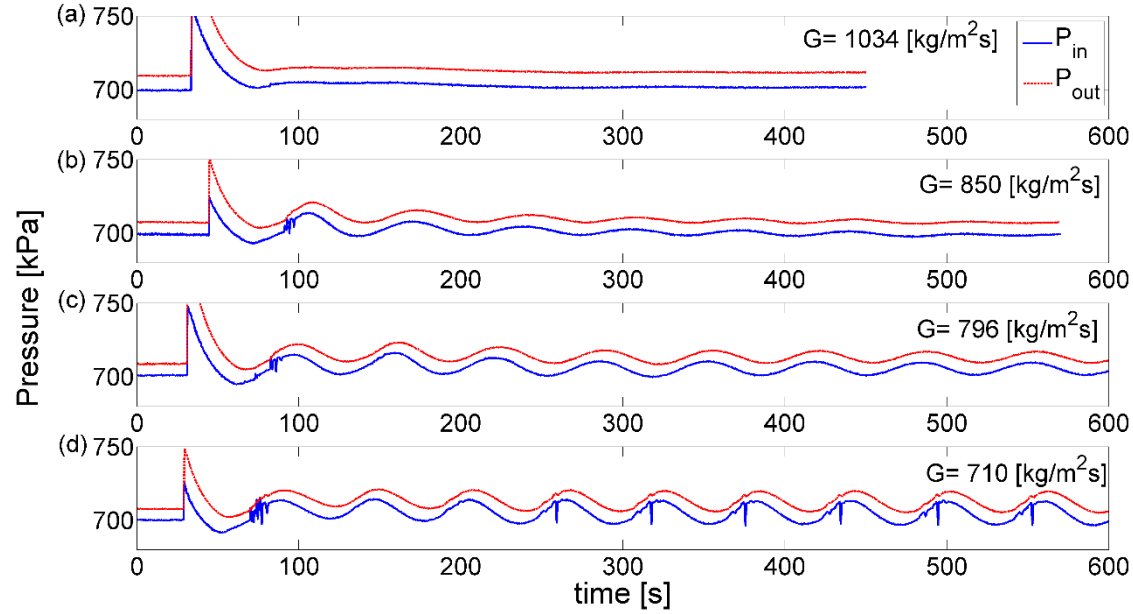

Figure 7. Trend of the pressure in different modes of instabilities (T_{sub} = 40.0 K)

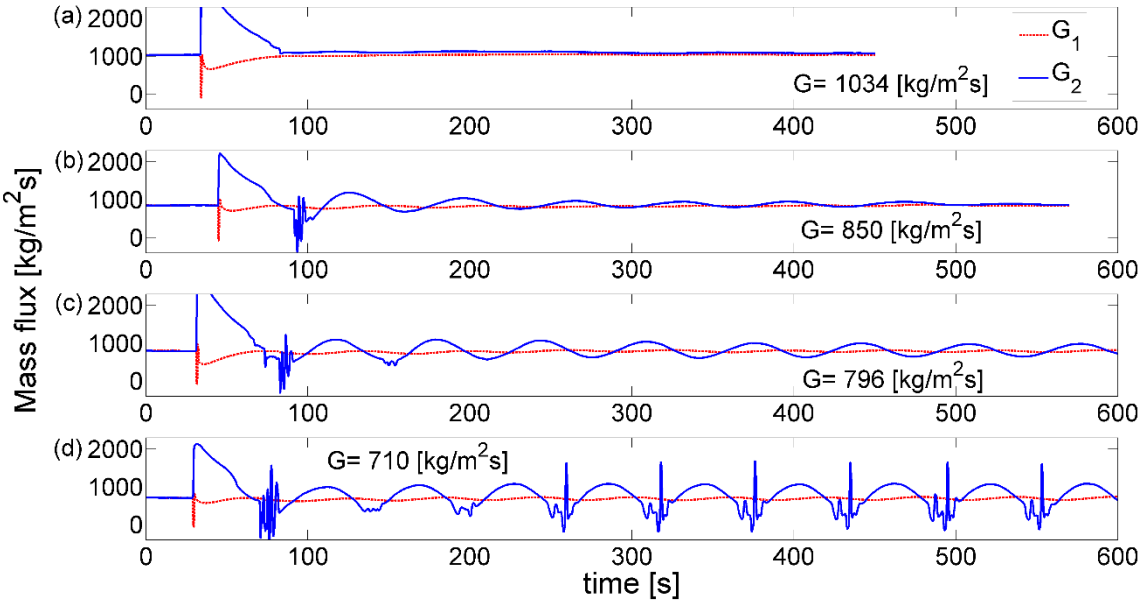

Figure 8. Trend of the mass flux in different modes of instabilities (T_{sub} = 40.0 K)

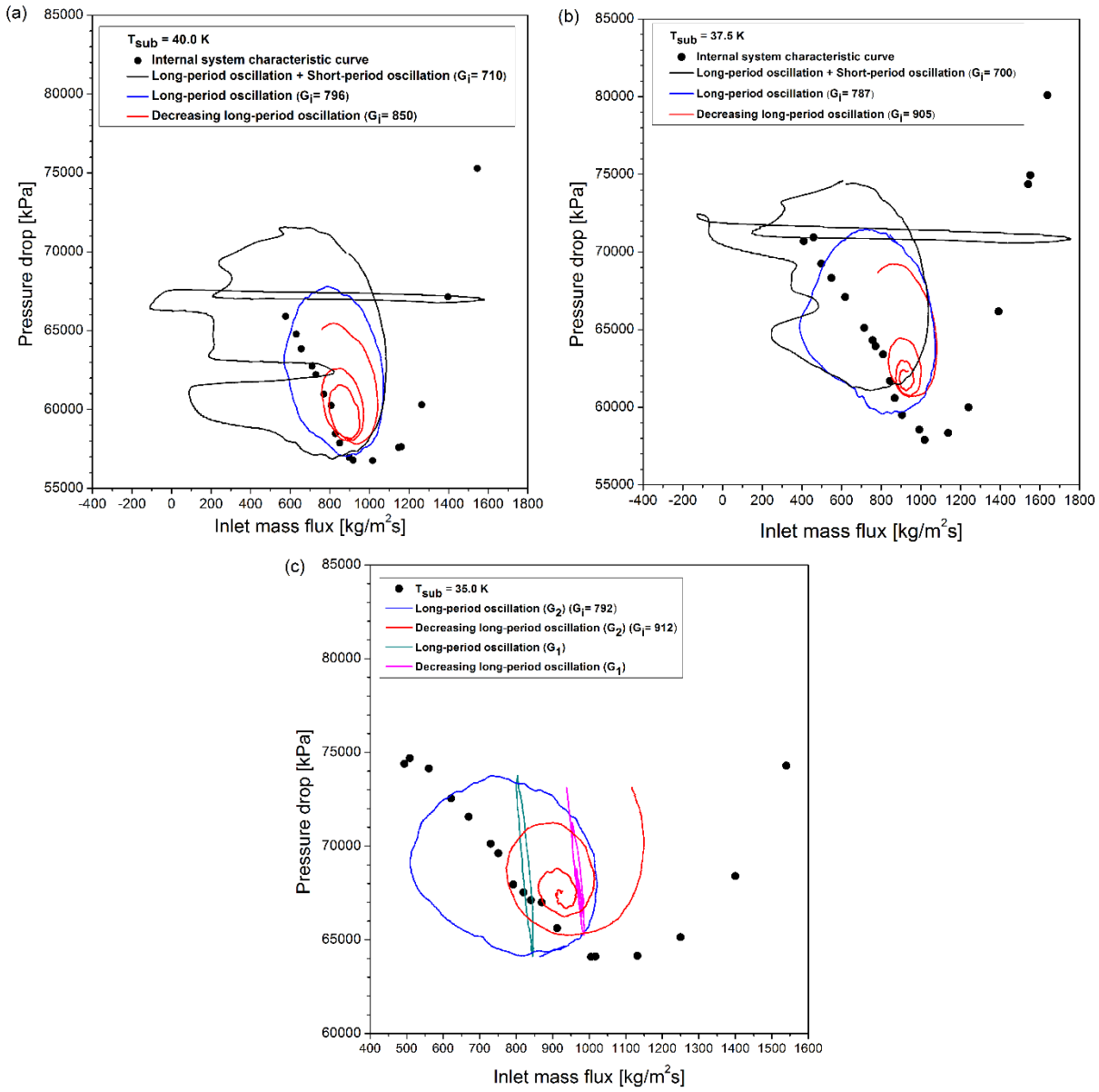

Figure 9. The limit cycle for different oscillation modes for different subcooling 40.0 K (a), 37.5 K (b), 35.0 K (c)

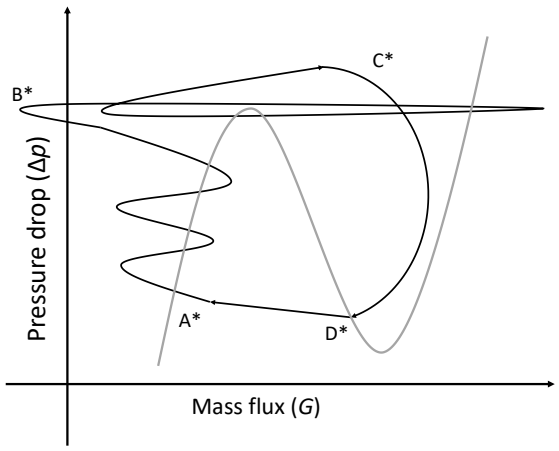

Figure 10. Schematic diagram for the mechanism of interaction between long-period oscillations and short-period oscillations from experimental data in this study.

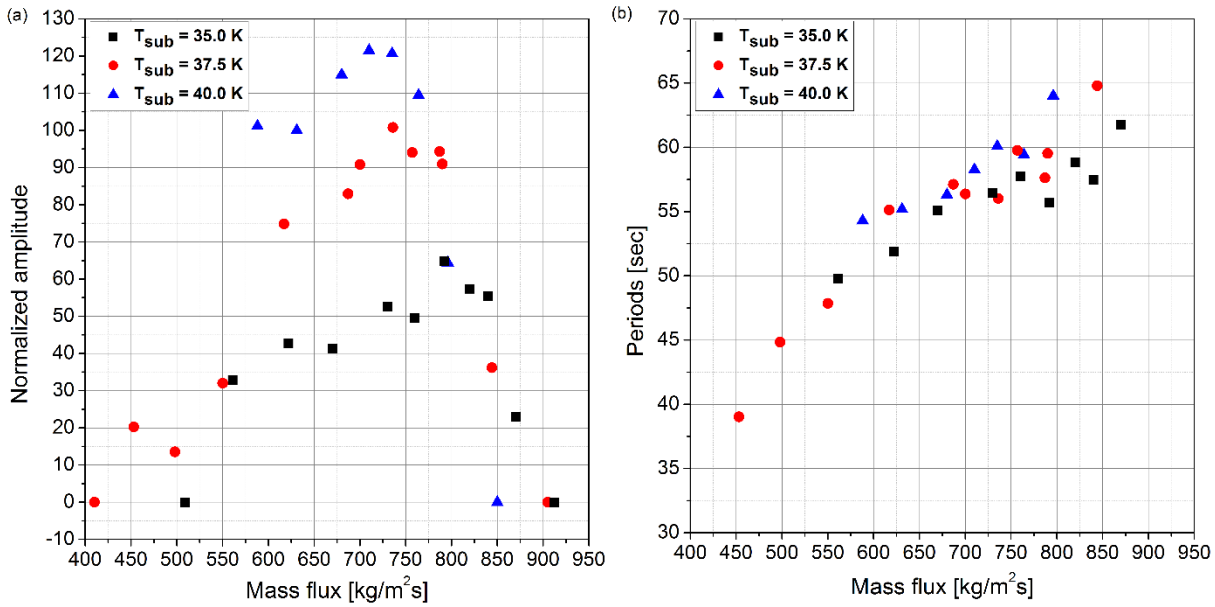

Figure 11. Effect on the amplitude (a) and the period (b) of PDOs

Table 2. Summary of effect on the amplitude and the period

Parameter	Author	Yüncü et al., 1991	Ding et al., 1995	Çomaklı et al., 2002	Park et al.
Increasing mass flow rate	Effect on the amplitude	No effect	Increase	Increase	Increase / Decrease
	Effect on the period	Decrease/ Increase	Increase	Increase	Increase
Increasing subcooling temperature	Effect on the amplitude	-	Increase	Increase	Increase / Decrease
	Effect on the period	-	Increase	Increase	Increase